Power Minimization Based Robust OFDM Radar Waveform Design for Radar and Communication Systems in Coexistence

Chenguang Shi, Fei Wang, Mathini Sellathurai, *Senior Member, IEEE,* Jianjiang Zhou, *Member, IEEE* and Sana Salous, *Senior Member, IEEE*

***Abstract*—This paper considers the problem of power minimization based robust orthogonal frequency division multiplexing (OFDM) radar waveform design, in which the radar coexists with a communication system in the same frequency band. Recognizing that the precise characteristics of target spectra are impossible to capture in practice, it is assumed that the target spectra lie in uncertainty sets bounded by known upper and lower bounds. Based on this uncertainty model, three different power minimization based robust radar waveform design criteria are proposed to minimize the worst-case radar transmitted power by optimizing the OFDM radar waveform, which are constrained by a specified mutual information (MI) requirement for target characterization and a minimum capacity threshold for communication system. These criteria differ in the way the communication signals scattered off the target are considered: (i) as useful energy, (ii) as interference or (iii) ignored altogether at the radar receiver. Numerical simulations demonstrate that the radar transmitted power can be efficiently reduced by exploiting the communication signals scattered off the target at the radar receiver. It is also shown that the robust waveforms bound the worst-case power-saving performance of radar system for any target spectra in the uncertainty sets.**

***Index Terms*—Radar waveform design, mutual information (MI), orthogonal frequency division multiplexing (OFDM), uncertainty model, power minimization.**

I. Introduction

A. Background and Motivation

In recent years, radar waveform design in spectrally dense environments has become a very challenging and essential problem. Traditional solutions to the radio frequency (RF) spectrum congestion call for the radar and wireless communication systems to be widely separated in the frequency band such that they do not interfere with each other [1]-[3]. However, it is still a problem today due to services with high bandwidth requirements and the exponential increase in the number of wireless devices. As such, various schemes such as waveform optimization, dynamic spectrum sensing and management can be adopted by either radar or communication systems for spectrum sharing [4]-[6]. The coexistence between radar and communication systems has been regarded as a promising solution which can replace traditional spectrum access approaches [7]. In such case, the radar and communication systems operate in the same frequency bandwidth, without causing too much interference to each other.

In terms of sharing the same frequency bandwidth, multicarrier waveforms are taken into account to be amongst the best candidates for both the radar and communication systems [8], which can bring several advantages over single carrier waveforms in radar system [9]-[11]. Motivated by the recent interest in multicarrier waveforms for radar system, the work in [12] develops a new mechanism for spectrum sharing between radar and orthogonal frequency division multiplexing (OFDM) communication systems, which allocates the subcarriers based on the importance of each channel. Bica et al. propose the radar waveform optimization algorithms for spectrum sharing based on target detection [13] and characterization [14], which show that the radar detection performance can be improved by exploiting the communication signals scattered off the target at the radar receiver. More recently, the novel bounds on performance of the joint system are defined in [15]. Reference [16] proposes a cooperative spectrum sharing scheme, where the MIMO radar transmit precoder and the communication transmit covariance matrix are jointly designed to optimize the radar signal-to-interference-plus-noise ratio (SINR) while guaranteeing certain rate for the communication system. The authors in [17] present a novel radar-embedded communication framework based on the remodulation of the incident radar signalling. Later, a multi-objective optimization paradigm based waveform design procedure is proposed in [18][19], where the symbol error rate and the intercept metric of the designed waveform are evaluated. Overall, the previous studies lay a solid foundation for the problem of radar and communication systems in coexistence, and it's worth mentioning that the radar system performance can be improved by optimizing the multicarrier radar waveform while guaranteeing the quality of communication links.

Manuscript revised September 22, 2017. This work was supported in part by the National Natural Science Foundation of China (Grant No. 61371170, No. 61671239, No. 61501228), in part by the Natural Science Foundation of Jiangsu Province (Grant No. BK20140825), in part by the Priority Academic Program Development of Jiangsu Higher Education Institutions (PADA) and in part by Key Laboratory of Radar Imaging and Microwave Photonics (Nanjing Univ. Aeronaut. Astronaut.), Ministry of Education, Nanjing University of Aeronautics and Astronautics, Nanjing, 210016, China. Finally, C. G. Shi wants to thank, in particular, the invaluable support received from his wife, Ying Hu over the years. (*Corresponding author: F. Wang.*)

C. G. Shi, F. Wang, and J. J. Zhou are with Key Laboratory of Radar Imaging and Microwave Photonics, Ministry of Education, Nanjing University of Aeronautics and Astronautics, Nanjing 210016, China.

M. Sellathurai is with the School of Engineering and Physical Sciences, Herriot Watt University, Edinburgh EH14 4AS, U.K..

S. Salous is with the School of Engineering and Computing Sciences, Durham University, Durham DH1 3LE, U.K..

B. Brief Survey of Similar Work

Information theory was applied to radar systems by Woodward for the first time in the early 1950s [20]. While the information-theoretic radar waveform design was pioneered by Bell with his seminal work [21], and the mutual information (MI) was utilized as a performance metric for target estimation. After that, the research in [22] studies the waveform design for multiple-input multiple-output (MIMO) radar by optimizing MI and minimum mean-square error (MMSE), showing that these two criteria yield the same optimum solution. Signal-to-noise ratio (SNR) and MI based matched illumination waveform design approaches for extended target are developed in [23][24]. Other existing works can refer to [25][26].

The radar waveform design for extended target requires the information of the target spectrum and the clutter statistics. In reality, the estimation of the clutter characteristics are formed by the receiver through previous received signals before the target appears [27]. While the spectra of the target of interest corresponding to various incident and scattered directions and polarized types can be stored in a database through electromagnetic modeling and calculation, which are obtained based on the target-radar orientation. However, the prefect target spectra are usually not available because the exact target-radar orientation is practically imprecise [28][29]. Some literatures adopt robust methods to design radar waveform in the presence of parameter uncertainty [30][31].

Although the reported studies provide us guidances to deal with the problem of optimal and robust radar waveform design, they are all addressed solely for the radar system. For the coexistence of a monostatic radar with a communication system operating in the same frequency band, the formulations and limitations are far more complicated. On the other hand, it is necessary to dynamically manage the radar resources to decrease its transmitted power for a given target estimation performance. Technically speaking, low transmit power, large sampling interval, and waveform agility will decrease the power consumption of radar system [32]. In [7],[13], and [14], the probability of detection and MI are maximized by optimizing OFDM radar waveform with a minimum capacity constraint for communication system respectively. While the algorithms do not concentrate on power minimization for radar system, and the effect of the signal-dependent clutter is ignored [34]-[36]. On the other hand, in [37], the low probability of intercept (LPI) based radar waveform optimization in signal-dependent clutter and white Gaussian noise for joint radar and communication systems are presented for the first time, where the radar transmit power is minimized for a predefined SINR threshold. However, these early works assume that the precise target spectra are available, which are no longer valid in the presence of target spectra uncertainties. In this paper, we will extend the result in [37] and the problem we will investigate is how to design robust waveform for a radar coexisted with a communication system in clutter and colored noise. To the best of our knowledge, the problem of power minimization based robust OFDM radar waveform design for spectrum sharing has not been fully considered until now.

C. Major Contributions

The major contributions of this work are fivefold:

(1) *Various expressions of MI between the received echoes from the target at the radar receiver and the target impulse response are derived to characterize the radar characterization performance, which incorporates the radar transmitted signals, the communication signals, the target spectra, the power spectral densities (PSDs) of signal-dependent clutters and colored noise.* These expressions of MI differ in the way the scattering off the target due to the communication signals is considered: (i) as useful energy, (ii) as interference or (iii) ignored altogether at the radar receiver.

(2) *Recognizing that the exact precise knowledge of target spectra is not available in realistic scenarios, the target spectra are assumed to lie in uncertainty sets bounded by known upper and lower bounds.*

(3) *The problem of power minimization based robust OFDM radar waveform design for the coexisting radar and communication systems in signal-dependent clutter and colored noise is studied.* It is assumed that the second order statistics of the communication signals and the PSDs of clutters are known by the radar. Based on the uncertainty model, three associated OFDM radar waveform design criteria are proposed to minimize the worst-case radar transmit power with a predefined MI constraint for target characterization and a minimum required capacity for communication system.

(4) *All the radar waveform design strategies are convex and solved analytically, and the bisection search technique is employed to find the optimal solutions for the aforementioned robust problems.* It is shown that remarkable computational savings are obtained through the use of bisection method when compared with the exhaustive search approach [37].

(5) Numerical results demonstrate the significance of exploiting the communication signals scattered off the target to decrease the power consumption of radar system via Monte Carlo simulations. In addition, we also reveal that the robust waveforms bound the worst-case power-saving performance of radar system for any target spectra in the uncertainty sets.

D. Outline of the Paper

The rest of this paper is organized as follows. The considered system model as well as the underlying assumptions needed in this paper are introduced in Section II. In Section III, the power minimization based optimal OFDM radar waveform design criteria are proposed given perfect knowledge of target spectra. In Section IV, the robust waveform design methods are presented, where the true target spectra are known only to lie in the uncertainty sets bounded by known upper and lower bounds. Numerical simulations are provided in Section V. Finally, Section VI concludes this paper with potential future work.

Notation: The continuous time domain signal is denoted by $x(t)$; the frequency domain representation of a discrete sample is $X[k]$. A single lower capital bold letter $\mathbf{x}$ represents a column vector with a given dimension, while an upper capital bold letter $\mathbf{X}$ represents a matrix. By x_k or $x[k]$ we denote the kth element of a vector $\mathbf{x}$. $\mathbb{E}\{\cdot\}$ represents the expectation

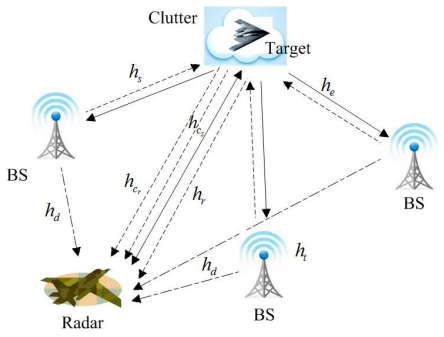

Fig. 1. Illustration of the system model.

operator. The symbol $*$ signifies the convolution operator. The symbol $\circ$ denotes the Hadamard product. The superscript $(\cdot)^T$ and $(\cdot)^*$ indicate transpose and optimality.

II. System and Signal Models

A. Problem Scenario

Let us consider a scenario, where one monostatic radar coexists with multiple communication base stations (BSs) aiming at tracking a target [14], as depicted in Fig.1. The channels of interest are given as follows: h_r for the radar-target-radar path, h_s for the BS-target-radar path, h_d for the direct BS-radar path, h_{c_s} for the radar-clutter-radar path, h_{c_r} for the BS-clutter-radar path, h_e for the radar-target-BS path, h_c for the communication channel inside a BS cell. Without loss of generality, this paper will concentrate on a single communication BS. However, the model and the derivations can be easily extended to N_t communication BSs [37].

To increase the spectral efficiency, we consider the co-existence of radar and communication systems in the same frequency band. The radar works with an antenna directed to the communication BS to receive the communication signal, and another one illuminates the target to receive the scattered echoes. Thus, the radar can receive the echo scattered from the target due to the transmitted radar signals as well as the communication signals from the BSs, via two channels: a direct path and a path which is due to scattering off the target. It is assumed that the channels are stationary over the observation period. The communication system carries out its task of data transmission by broadcasting signals throughout the space. In addition, it is assumed that the radar antenna is directional and steered towards the target, thus the target signal does not arrive at the communication systems through a direct path, but only scatters off the target.

B. Signal Model

It is assumed that both the radar and the communication systems use OFDM-type multicarrier signals with K subcarriers. The deterministic radar signal $x_r(t)$ is given by [7]:

$$x_r(t) = \frac{1}{\sqrt{K}} \sum_{k=0}^{K-1} u_k e^{j2\pi(f_c + k\Delta f)t}, \tag{1}$$

where u_k denotes the amplitude of the kth subcarrier of radar signal, f_c denotes the carrier frequency, and Δf denotes the subcarrier spacing. The matrix formulation for the discrete time version of (1) is [8]:

$$\mathbf{X}_r = \mathbf{Q}_K \mathbf{U}, \tag{2}$$

where $\mathbf{Q}_K$ is a $K \times K$-dimensional inverse discrete Fourier transform (IDFT) matrix

$$\mathbf{Q}_K = \frac{1}{\sqrt{K}} \begin{bmatrix} 1 & 1 & \cdots & 1 \\ 1 & Q_K & \cdots & Q_K^{K-1} \\ 1 & Q_K^2 & \cdots & Q_K^{2(K-1)} \\ \vdots & \vdots & \ddots & \vdots \\ 1 & Q_K^{K-1} & \cdots & Q_K^{(K-1)(K-1)} \end{bmatrix} \tag{3}$$

with $Q_K = e^{j2\pi/K}$. $\mathbf{U} = [u_0, u_1, \cdots, u_{K-1}]^T$ is a $K \times 1$ vector that contains the weights of all subcarriers. Here, all-cell Doppler correction (ACDC) method is employed to enable an inter-carrier-interference (ICI) free processing for OFDM systems [38]. With this approach, the cyclic prefix can be omitted. Hence, it is a highly valuable feature for radar applications with dynamic targets and long range of interest. Moreover, the radar transmitted energy can be continuously received and processed, which improves the SNR and energy efficiency of OFDM radar system. Refer to [38] for details.

For the communication BS, the transmitted signal $x_s(t)$ is:

$$x_s(t) = \frac{1}{\sqrt{K}} \sum_{k=0}^{K-1} w_k e^{j2\pi(f_c + k\Delta f)t}, \tag{4}$$

where w_k is the amplitude of the kth subcarrier of communication signal. Without loss of generality, it is assumed that the w_k are statistically independent, identically distributed (i.i.d.) random variables with zero mean and variance $\sigma_{x_s}^2 \triangleq \mathbb{E}\{|w_k|^2\}$ for large number of subcarriers by the central limit theorem [39] (See more details in [39]). Thus, the baseband communication signal $x_s(t)$ of (4) converges to a complex Gaussian random process with zero mean and variance $\sigma_{x_s}^2$ for large K, and the variance of the communication signal, that is, the power of the communication signal, is known at the radar receiver after a previous estimation step [40]. The autocorrelation function of $x_s(t)$ can be written as $R(\tau) = \sigma_{x_s}^2 \delta(\tau)$, where $\delta(\cdot)$ denotes Dirac function, $\tau = t_2 - t_1$ denotes the time difference between time slot t_2 and t_1. Likewise, the matrix formulation of the discrete time version of (4) is:

$$\mathbf{X}_s = \mathbf{Q}_K \mathbf{W}, \tag{5}$$

where $\mathbf{W} = [w_0, w_1, \cdots, w_{K-1}]^T$. Also, ACDC is applied for communication system analogous to radar.

Generally speaking, OFDM systems are much more sensitive to timing and frequency offset than single-carrier systems. Hence, timing and frequency synchronization is one important step that must be designed for these systems [41]. Several timing and frequency synchronization techniques have been presented in the literature, which are either training data aided [42]-[45] or simply blind [41], [46]-[48]. The second scheme, which is also known as non-data aided, is power efficient or bandwidth efficient and can be utilized when the cyclic prefix is absent. Therefore, the radar and communication systems can be synchronized in terms of timing and frequency. It

is also supposed that the radar and communication systems have the same symbol duration. This enables an inter-symbol-interference (ISI) free processing between radar and communication signals. In case of a monostatic radar and a communication BS, the received signal at the radar receiver can be expressed in the continuous time domain as:

$$y(t) = r(t) + [r_s(t) + s(t) + r_{c_s}(t)] + r_{c_r}(t) + n(t), \quad (6)$$

where $y(t)$ denotes the received signal at the radar receiver, $r(t)$ is the echo from the target due to the transmitted radar signal, $r_s(t)$ is the scattering off the target due to communication signal, $s(t)$ is the communication signal arriving through a direct line of sight path at the radar receiver. $r_{c_s}(t)$ is the complex-valued, zero-mean Gaussian random process representing the signal-dependent clutter due to the communication signal, $r_{c_r}(t)$ is the complex-valued, zero-mean Gaussian random clutter due to the radar signal and $n(t)$ is the additive colored noise with known variance. Thus, for a single communication system, (6) can be rewritten as:

$$\begin{aligned} y(t) =& x_r(t) * h_r(t) + [x_s(t) * h_s(t) + x_s(t) * h_d(t) \\ &+ x_s(t) * h_{c_s}(t)] + x_r(t) * h_{c_r}(t) + n(t). \end{aligned} \quad (7)$$

It is indicated in [21] that an extension for the delay-Doppler case is possible, but it complicates the formulation. Then, the discrete time version of (7) can be written in matrix formulation as follows [8]:

$$\begin{aligned} \mathbf{y} =& \mathbf{Q}_K(\mathbf{H}_r \circ \mathbf{L}_r^{1/2})\mathbf{U} + [\mathbf{Q}_K(\mathbf{H}_s \circ \mathbf{L}_s^{1/2})\mathbf{W} + \mathbf{Q}_K\mathbf{L}_d^{1/2}\mathbf{W} \\ &+ \mathbf{Q}_K(\mathbf{H}_{c_s} \circ \mathbf{L}_{c_s}^{1/2})\mathbf{W}] + \mathbf{Q}_K(\mathbf{H}_{c_r} \circ \mathbf{L}_{c_r}^{1/2})\mathbf{U} + \mathbf{n}, \end{aligned} \quad (8)$$

where $\mathbf{y}$ represents a $K \times 1$ vector corresponding to the signal at the radar receiver, $\mathbf{n}$ is modeled as the colored noise with zero mean and known variance, the $K \times K$ diagonal matrices $\mathbf{H}_r$ and $\mathbf{H}_s$ denote the corresponding target spectra:

$$\begin{cases} \mathbf{H}_r = \text{diag}\left\{H_r[0], H_r[1], \cdots, H_r[K-1]\right\}, \\ \mathbf{H}_s = \text{diag}\left\{H_s[0], H_s[1], \cdots, H_s[K-1]\right\}, \end{cases} \quad (9)$$

where $H_r[k]$ and $H_s[k]$ denote the target spectra for the radar-target-radar path and the BS-target-radar path at the kth subcarrier, respectively. $\mathbf{H}_{c_s}$ and $\mathbf{H}_{c_r}$ represent the clutter frequency responses due to communication and radar signals:

$$\begin{cases} \mathbf{H}_{c_s} = \text{diag}\left\{H_{c_s}[0], H_{c_s}[1], \cdots, H_{c_s}[K-1]\right\}, \\ \mathbf{H}_{c_r} = \text{diag}\left\{H_{c_r}[0], H_{c_r}[1], \cdots, H_{c_r}[K-1]\right\}, \end{cases} \quad (10)$$

where $H_{c_s}[k]$ and $H_{c_r}[k]$ denote the corresponding complex-valued, zero-mean Gaussian random processes for the kth subcarrier, and characterized by the PSDs $P_{c_s}[k]$ and $P_{c_r}[k]$. The matrices $\mathbf{L}_r$, $\mathbf{L}_s$, $\mathbf{L}_d$, $\mathbf{L}_{c_s}$, and $\mathbf{L}_{c_r}$ represent the propagation losses of the corresponding channels [49]:

$$\begin{cases} \mathbf{L}_r = \text{diag}\left\{L_r[0], L_r[1], \cdots, L_r[K-1]\right\} \\ \quad = \mathbf{L}_{c_r} = \text{diag}\left\{L_{c_r}[0], L_{c_r}[1], \cdots, L_{c_r}[K-1]\right\} \\ \quad = \text{diag}\left\{\dfrac{G_tG_r\lambda_0^2}{(4\pi)^3 d_r^4}, \cdots, \dfrac{G_tG_r\lambda_{K-1}^2}{(4\pi)^3 d_r^4}\right\}, \\ \mathbf{L}_s = \text{diag}\left\{L_s[0], L_s[1], \cdots, L_s[K-1]\right\} \\ \quad = \mathbf{L}_{c_s} = \text{diag}\left\{L_{c_s}[0], L_{c_s}[1], \cdots, L_{c_s}[K-1]\right\} \\ \quad = \text{diag}\left\{\dfrac{G_sG_r\lambda_0^2}{(4\pi)^3 d_s^2 d_r^2}, \cdots, \dfrac{G_sG_r\lambda_{K-1}^2}{(4\pi)^3 d_s^2 d_r^2}\right\}, \\ \mathbf{L}_d = \text{diag}\left\{L_d[0], L_d[1], \cdots, L_d[K-1]\right\} \\ \quad = \text{diag}\left\{\dfrac{G_sG_r\lambda_0^2}{(4\pi)^2 d_b^2}, \cdots, \dfrac{G_sG_r\lambda_{K-1}^2}{(4\pi)^2 d_b^2}\right\}, \end{cases} \quad (11)$$

where G_t is the transmit antenna gain of the radar system, G_r is the receive antenna gain of the radar system, G_s is the antenna gain of the communication system, λ_k is the wavelength at kth subcarrier. We let d_r, d_s, and d_b denote the distances between the radar and the target, between the communication system and the target, and between the radar and the communication system, respectively.

Remark 1: From a practical stand point, one of the major disadvantages of OFDM waveform is the high peak-to-average power ratio (PAPR), which leads to nonlinear distortion of the signal, ICI, and radar performance degradation due to the limited linear region of the power amplifier [50]. Over the years, there have been a number of proposed techniques to minimize the PAPR by phase modulation transform, block coding, etc., which make it possible to implement the OFDM radar waveform in reality. The OFDM waveform design taking into account the PAPR will be investigated in the future.

III. Optimal OFDM Radar Waveform Design

A. Basic of the Technique

Mathematically, the power minimization based optimal radar waveform design can be formulated as a problem of optimizing OFDM radar waveform to minimize the radar transmitted power subject to some system constraints. Firstly, three different expressions of MI between the received echoes from the target at the radar receiver and the target impulse response are derived, which differ in the way the communication signals scattered off the target are considered: (i) as useful energy, (ii) as interference or (iii) ignored altogether at the radar receiver. We are then in a position to design the radar waveform in order to minimize the power consumption of radar system. The general power minimization based optimal OFDM radar waveform design strategies are detailed as follows.

B. Optimal Radar Waveform Design Criterion 1

As implied in [8][21], the MI between the received echo and the target impulse response can be utilized as a metric for target characterization performance in the radar system. It is assumed that the target spectra at different subcarriers are independent and both $\mathbf{H}_r$ and $\mathbf{H}_s$ partly contain information about the target, since the radar signals and the communication

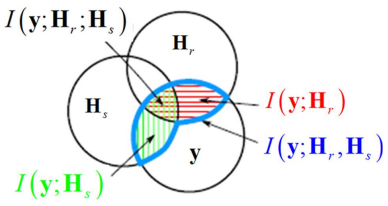

Fig. 2. Venn diagram of information theoretic measures for $\mathbf{y}$, $\mathbf{H}_r$ and $\mathbf{H}_s$. The area with the horizontal red stripes and vertical green stripes corresponds to $I(\mathbf{y};\mathbf{H}_r;\mathbf{H}_s)$, which denotes the multivariate MI between $\mathbf{y}$, $\mathbf{H}_r$ and $\mathbf{H}_s$. The areas with the horizontal red stripes and vertical green stripes correspond to $I(\mathbf{y};\mathbf{H}_r)$ and $I(\mathbf{y};\mathbf{H}_s)$, respectively. The area with only the horizontal red stripes corresponds to $I(\mathbf{y};\mathbf{H}_r|\mathbf{H}_s)$. The area with only the vertical green stripes corresponds to $I(\mathbf{y};\mathbf{H}_s|\mathbf{H}_r)$.

signals illuminate a common area of the target [14]. Fig.2 illustrates the Venn diagram of information theoretic measures for the received signal at the radar receiver $\mathbf{y}$ and the target impulse responses associated with the radar signal $\mathbf{H}_r$ and the communication signal $\mathbf{H}_s$. Thus, the achievable MI between $\mathbf{y}$ and, jointly, $\mathbf{H}_r$ and $\mathbf{H}_s$ which is marked by the thicker blue line in Fig.2, can be posed as (12), shown at the top of the next page [14][24].

In (12), $U[k]$ denotes the amplitude of the kth subcarrier of radar signal in frequency domain, $|U[k]|^2$ and $\sigma_{x_s}^2[k]$ are the power of the radar and communication signals for the kth subcarrier respectively. $\sigma_n^2[k]$ is the power of the radar recevier noise for the kth subcarrier. It should be pointed out from (12) that the communication signals scattered off the target is considered as useful energy. In this case, we can notice that the achievable MI is related to the radar transmitted waveform, the target spectra, the communication waveform, the PSDs of the signal-dependent clutters, and the propagation losses of corresponding channels. Intuitively, maximization of MI means better radar estimation performance, while it also leads to higher power consumption in hostile environments.

Herein, we concentrate on the power minimization based optimal OFDM radar waveform design for the coexisting radar and communication system, whose purpose is to minimize the radar transmitted power for a predefined target characterization performance. We impose a minimum capacity constraint per channel for the communication system and for the radar signal an upper bound on the transmit power per channel. Eventually, the optimal radar waveform optimization can be formulated as (13), where $\mathcal{F}_k \triangleq \{0, 1, \cdots, K-1\}$ is the index-set of all K subcarriers, $\sigma_s^2[k]$ is the variance of white Gaussian noise at communication BS. The first constraint stands that the achieved MI is greater than a given MI threshold MI_{min} such that the required target estimation performance is met, while the second one stands that the capacity of the kth subcarrier in communication system should be above the threshold t_k to guarantee the communication performance, which can be provided by the communication system. It is worth mentioning that if the communication system is not accessible, the threshold t_k cannot be obtained by the radar. However, the radar waveform can still be designed based on the received communication signal. In this case, the symbol error rate (SER) can be calculated as indicated in [6]. The communication receiver works well as if no radar signal is present. It has been demonstrated that the SER of the communication system coexisted with a radar is approximately zero in the simulation scenario, which is not shown due to the limited space. The third constraint represents that the transmit power for the kth subcarrier is limited by a maximum value $P_{\text{max},k}$ and a minimum value 0. $H_e[k]$ is the target spectrum for the radar-target-BS path. $L_c[k]$ and $L_e[k]$ represent the propagation losses of the corresponding channels:

$$\begin{cases} L_c[k] = \dfrac{G_s^2 \lambda_k^2}{(4\pi)^2 d_c^2}, \\ L_e[k] = \dfrac{G_t G_s \lambda_k^2}{(4\pi)^3 d_r^2 d_s^2}, \end{cases} \tag{14}$$

where d_c is the radius of communication cell. The minimum capacity constraint for the communication system is considered inside a cell. The interference is represented by the radar signals that are scattered off the target and arrive inside the cell. After simplifying the constraints and making the notation $x_k = |U[k]|^2$, we can rewrite problem (15) as follows:

$$\mathcal{P}_{\text{O-1}}: \quad \min_{x_k, k\in\mathcal{F}_k} \sum_{k=0}^{K-1} x_k, \tag{15a}$$

$$\text{s.t.}: \begin{cases} \displaystyle\sum_{k=0}^{K-1} \log\left(1 + \frac{m_k x_k + a_k}{n_k x_k + b_k}\right) \geq \text{MI}_{\text{min}}, \\ \mathbf{0} \leq \mathbf{x} \leq \mathbf{d}. \end{cases} \tag{15b}$$

where we define:

$$\begin{cases} a_k = \sigma_{x_s}^2[k]|H_s[k]|^2 L_s[k], \\ b_k = \sigma_{x_s}^2[k] L_d[k] + \sigma_{x_s}^2[k] P_{c_s}[k] L_{c_s}[k] + \sigma_n^2[k], \\ c_k = \dfrac{1}{|H_e[k]|^2 L_e[k]} \left[\dfrac{\sigma_{x_s}^2[k] L_c[k]}{e^{t_k} - 1} - \sigma_s^2[k]\right], \\ d_k = \min\left\{P_{\text{max},k}, c_k\right\}, \\ m_k = |H_r[k]|^2 L_r[k], \\ n_k = P_{c_r}[k] L_{c_r}[k]. \end{cases} \tag{16}$$

Lemma 1: The optimization problem $\mathcal{P}_{\text{O-1}}$ is convex.

Proof: The proof is provided in Appendix.

Theorem 1: Suppose perfect knowledge of target spectra is available. Define

$$\begin{cases} A_k = (m_k + n_k) n_k, \\ B_k = (m_k + n_k) b_k + (a_k + b_k) n_k, \\ C_k = (a_k + b_k) b_k, \\ D_k = b_k m_k - a_k n_k. \end{cases} \tag{17}$$

Then, under a predefined MI threshold and a minimum capacity requirement for the communication system, the optimal OFDM radar waveform corresponding to $\mathcal{P}_{\text{O-1}}$ that minimizes the total transmitted power should satisfy (18), shown at the top of the next page, where λ_3^* is a constant determined by the given MI constraint:

$$\sum_{k=0}^{K-1} \log\left(1 + \frac{m_k x_k^* + a_k}{n_k x_k^* + b_k}\right) \geq \text{MI}_{\text{min}}. \tag{19}$$

$$\begin{aligned}\mathcal{I}_{\text{optimal}}(\mathbf{y};\mathbf{H}_r,\mathbf{H}_s) &\triangleq H(\mathbf{y}) - H(\mathbf{y}|\mathbf{H}_r,\mathbf{H}_s)\\ &= \sum_{k=0}^{K-1}\log\left(1+\frac{|U[k]|^2|H_r[k]|^2L_r[k]+\sigma_{x_s}^2[k]|H_s[k]|^2L_s[k]}{|U[k]|^2P_{c_r}[k]L_{c_r}[k]+\sigma_{x_s}^2[k]L_d[k]+\sigma_{x_s}^2[k]P_{c_s}[k]L_{c_s}[k]+\sigma_n^2[k]}\right),\end{aligned} \tag{12}$$

$$\min_{X_r[k],k\in\mathcal{F}_k}\ \sum_{k=0}^{K-1}|U[k]|^2, \tag{13a}$$

$$\text{s.t.}:\ \begin{cases}\displaystyle\sum_{k=0}^{K-1}\log\left(1+\frac{|U[k]|^2|H_r[k]|^2L_r[k]+\sigma_{x_s}^2[k]|H_s[k]|^2L_s[k]}{|U[k]|^2P_{c_r}[k]L_{c_r}[k]+\sigma_{x_s}^2[k]L_d[k]+\sigma_{x_s}^2[k]P_{c_s}[k]L_{c_s}[k]+\sigma_n^2[k]}\right)\geq \text{MI}_{\min},\\ \displaystyle\log\left(1+\frac{\sigma_{x_s}^2[k]L_c[k]}{|U[k]|^2|H_e[k]|^2L_e[k]+\sigma_s^2[k]}\right)\geq t_k,\\ 0\leq|U[k]|^2\leq P_{\max,k}.\end{cases} \tag{13b}$$

$$x_k^*=\begin{cases}0, & \lambda_3^*D_k-C_k\leq 0,\\ -\frac{B_k}{2A_k}+\frac{1}{2A_k}\sqrt{B_k^2-4A_k(C_k-\lambda_3^*D_k)}, & 0<\lambda_3^*D_k-C_k<A_kd_k^2+B_kd_k,\\ d_k, & \lambda_3^*D_k-C_k\geq A_kd_k^2+B_kd_k.\end{cases} \tag{18}$$

Proof: The problem $\mathcal{P}_{\text{O-1}}$ can be solved by utilizing the method of Lagrange multipliers, which is omitted here for brevity. Refer to [37] for detailed proof.

Remark 2: As it reasonably arises, our solution scheme is to choose λ_3^* as a search variable, and use the result (18) to identify the optimal power allocation for all the subcarriers. The well-known bisection search approach [6] is employed to find the value of λ_3^*, which ensures the optimum transmit waveform x_k^* while making sure that the constraints are totally satisfied. The importance of the derived solution (18) lies in the fact that it provides an explicit relation between the power allocation in each subcarrier and the resulting value of λ_3^*. Criterion 1 defines a procedure which finally provides the optimal transmit power allocation, and consequently, the optimum power-saving performance. The iterative procedure is detailed in Algorithm 1. The bisection search algorithm is listed as Algorithm 2.

Remark 3: The problem of power minimization based optimal radar waveform design $\mathcal{P}_{\text{O-1}}$ given by (15) is convex, and the optimal OFDM waveform design results $\{x_k^*\}_{k=0}^{K-1}$ can be obtained by solving (15) for a specified MI constraint and a given set of transmit power. At the $(t+1)$th step, the designed waveforms $\{x_k^{(t+1)}\}_{k=0}^{K-1}$ are updated from the optimal solutions $\{x_k^{(t)}\}_{k=0}^{K-1}$ determined through the previous iteration. Hence, $\{x_k^{(t+1)}\}_{k=0}^{K-1}$ are always feasible solutions of the next iteration, and the optimal waveform design results $\{x_k^{(t+1)}\}_{k=0}^{K-1}$ will achieve an MI value, which is greater or equal to that of the previous iteration. This shows that the achieved MI value will monotonically increase at each iteration step, such that the gap between the temporal MI and the specified MI threshold is minimized. Thus, Algorithm 1 will converge to the optimal solutions through bisection search method, which is due to the fact that the achievable MI is upper bounded for a given set of transmit power at the radar transmitter.

Algorithm 1 : Optimal Waveform Design Criterion 1

1: **Initialization:** $\text{MI}_{\min}$, $P_{\max,k}$, iterative index $t=1$;
2: **Loop until** $\mathbf{x}$ **converges:**
  for k = 1, $\cdots$, K, **do**
    Calculate $x_k^{(t)}$ by solving (18);
    Calculate $\text{MI}^{(t)} \leftarrow \sum_{k=0}^{K-1}\log\left(1+\frac{m_kx_k^{(t)}+a_k}{n_kx_k^{(t)}+b_k}\right)$;
    Obtain $\lambda_3^{(t+1)}$ via bisection search in Algorithm 2;
  end for
3: **End loop**
4: **Update:** Update $x_k^* \leftarrow x_k^{(t)}$ for $\forall k$.

C. Optimal Radar Waveform Design Criterion 2

Next, we define the achievable MI between $\mathbf{y}$ and $\mathbf{H}_r$ as shown in (19) [see (19) at the top of the next page], which corresponds to the area with the horizontal red stripes and vertical green stripes in Fig.2.

One can see from (19) that the scattering off the target due to the communication signal is considered as interference. Similarly, the optimal radar waveform design approach is expressed as follows:

$$\mathcal{P}_{\text{O-2}}:\quad \min_{x_k,k\in\mathcal{F}_k}\ \sum_{k=0}^{K-1}x_k, \tag{20a}$$

$$\text{s.t.}:\ \begin{cases}\displaystyle\sum_{k=0}^{K-1}\log\left(1+\frac{m_kx_k}{n_kx_k+a_k+b_k}\right)\geq \text{MI}_{\min},\\ \mathbf{0}\leq\mathbf{x}\leq\mathbf{d}.\end{cases} \tag{20b}$$

$$\mathcal{I}_{\text{optimal}}(\mathbf{y};\mathbf{H}_r) \triangleq H(\mathbf{y}) - H(\mathbf{y}|\mathbf{H}_r) = \sum_{k=0}^{K-1} \log\left(1 + \frac{|U[k]|^2|H_r[k]|^2 L_r[k]}{|U[k]|^2 P_{c_r}[k]L_{c_r}[k] + \sigma_{x_s}^2[k]|H_s[k]|^2 L_s[k] + \sigma_{x_s}^2[k]L_d[k] + \sigma_{x_s}^2[k]P_{c_s}[k]L_{c_s}[k] + \sigma_n^2[k]}\right), \tag{19}$$

Algorithm 2 : Bisection Search of λ_3

1: **Initialization:** $\lambda_3^{(t)}$, $\lambda_{3,\max}$, $\lambda_{3,\min}$, the tolerance $\epsilon > 0$;
2: **Loop until:** $\text{MI}^{(t)} - \text{MI}_{\min} \geq \epsilon$
  for k = 1, $\cdots$, K, **do**
    $\lambda_3^{(t)} \leftarrow (\lambda_{3,\min} + \lambda_{3,\max})/2$;
    Calculate $x_k^{(t)}$ from (18) and update $\text{MI}^{(t)}$;
    if $\text{MI}^{(t)} > \text{MI}_{\min}$ **then**
      $\lambda_{3,\max} \leftarrow \lambda_3^{(t)}$;
      $\lambda_3^{(t)} \leftarrow (\lambda_{3,\min} + \lambda_{3,\max})/2$;
    else
      $\lambda_{3,\min} \leftarrow \lambda_3^{(t)}$;
      $\lambda_3^{(t)} \leftarrow (\lambda_{3,\min} + \lambda_{3,\max})/2$;
    end if
    Set $t \leftarrow t + 1$;
  end for
3: **End loop**

Theorem 2: Suppose perfect knowledge of target spectra is available. Define

$$\begin{cases} E_k = (m_k + 2n_k)(a_k + b_k), \\ F_k = (a_k + b_k)^2, \\ G_k = m_k(a_k + b_k). \end{cases} \tag{21}$$

Then, under a predefined MI threshold and a minimum capacity for the communication system, the optimal OFDM radar waveform corresponding to $\mathcal{P}_{\text{O-2}}$ that minimizes the total transmitted power should satisfy (22), shown at the top of the next page, where λ_3^* is determined by:

$$\sum_{k=0}^{K-1} \log\left(1 + \frac{m_k x_k^*}{n_k x_k^* + a_k + b_k}\right) \geq \text{MI}_{\min}. \tag{23}$$

The iterative procedure for problem $\mathcal{P}_{\text{O-2}}$ is similar to Algorithm 1, and thus the details are omitted here.

D. Optimal Radar Waveform Design Criterion 3

One can also choose the MI between $\mathbf{y}$ and $\mathbf{H}_r$, conditioned on $\mathbf{H}_s$, as shown in (24) [see (24) at the top of the next page], which corresponds to the area with only the horizontal red stripes in Fig.2. It can be seen from (24) that the scattering due to the communication signal is ignored. Proceeding as before, we can write the optimization problem as follows:

$$\mathcal{P}_{\text{O-3}}: \quad \min_{x_k, x\in\mathcal{F}_k} \sum_{k=0}^{K-1} x_k, \tag{25a}$$

$$\text{s.t.}: \begin{cases} \sum_{k=0}^{K-1} \log\left(1 + \frac{m_k x_k}{n_k x_k + b_k}\right) \geq \text{MI}_{\min}, \\ \mathbf{0} \leq \mathbf{x} \leq \mathbf{d}. \end{cases} \tag{25b}$$

Theorem 3: Suppose perfect knowledge of target spectra is available. Define

$$\begin{cases} H_k = b_k(m_k + 2n_k), \\ J_k = b_k^2, \\ L_k = m_k b_k. \end{cases} \tag{26}$$

Then, under a predefined MI threshold and a minimum capacity for the communication system, the optimal OFDM radar waveform corresponding to $\mathcal{P}_{\text{O-3}}$ that minimizes the total transmitted power should satisfy (27), shown at the top of the next page, where λ_3^* is determined by:

$$\sum_{k=0}^{K-1} \log\left(1 + \frac{m_k x_k^*}{n_k x_k^* + b_k}\right) \geq \text{MI}_{\min}. \tag{28}$$

The iterative procedure for $\mathcal{P}_{\text{O-3}}$ is also omitted here.

E. Discussion

1) Implication: Note that the MI (12), (19) and (24) have a similar expression as a function of radar transmit waveform x_k, which results in a similar structure between the target parameter estimation requirement constraints (15b), (20b) and (25b), and hence $\mathcal{P}_{\text{O-1}}$, $\mathcal{P}_{\text{O-2}}$ and $\mathcal{P}_{\text{O-3}}$. Thus, we can present the optimal OFDM radar waveform design algorithms for the three scenarios under a unifying framework. It should be noted from the SINR term of the MI expressions in (12), (19), and (24) that the reflections off the target due to the communication signals contribute to the signal part in (12), to the interference part in (19) and to neither in (24) [14].

2) Computational Complexity: The computational complexity of Algorithm 1 is dominated by the number of subcarriers and the procedure of bisection search method. The complexity of the loop inside the step 2 is $\mathcal{O}(K)$. The convergence rate of the step 2 is based on the bisection search method, which is given by $\mathcal{O}(\log_2[(\lambda_{3,\max} - \lambda_{3,\min})/\epsilon])$. Thus, the total complexity of Algorithm 1 is $\mathcal{O}(K\log_2[(\lambda_{3,\max} - \lambda_{3,\min})/\epsilon])$. In addition, Criteria 2 and 3 have the same computational complexity as Criterion 1, i.e., $\mathcal{O}(K\log_2[(\lambda_{3,\max} - \lambda_{3,\min})/\epsilon])$. While the exhaustive search [37] has a complexity of $\mathcal{O}(K(\lambda_3^* -$

$$x_k^* = \begin{cases} 0, & \lambda_3^* G_k - F_k \le 0, \\ -\frac{E_k}{2A_k} + \frac{1}{2A_k}\sqrt{E_k^2 - 4A_k(F_k - \lambda_3^* G_k)}, & 0 < \lambda_3^* G_k - F_k < A_k d_k^2 + E_k d_k, \\ d_k, & \lambda_3^* G_k - F_k \ge A_k d_k^2 + E_k d_k. \end{cases} \tag{22}$$

$$\begin{aligned} \mathcal{I}_{\text{optimal}}(\mathbf{y}; \mathbf{H}_r | \mathbf{H}_s) &\triangleq H(\mathbf{y}|\mathbf{H}_s) - H(\mathbf{y}|\mathbf{H}_r, \mathbf{H}_s) \\ &= \sum_{k=0}^{K-1} \log\left(1 + \frac{|U[k]|^2 |H_r[k]|^2 L_r[k]}{|U[k]|^2 P_{c_r}[k] L_{c_r}[k] + \sigma_{x_s}^2[k] L_d[k] + \sigma_{x_s}^2[k] P_{c_s}[k] L_{c_s}[k] + \sigma_n^2[k]}\right), \end{aligned} \tag{24}$$

$$x_k^* = \begin{cases} 0, & \lambda_3^* L_k - J_k \le 0, \\ -\frac{H_k}{2A_k} + \frac{1}{2A_k}\sqrt{H_k^2 - 4A_k(J_k - \lambda_3^* L_k)}, & 0 < \lambda_3^* L_k - J_k < A_k d_k^2 + H_k d_k, \\ d_k, & \lambda_3^* L_k - J_k \ge A_k d_k^2 + H_k d_k. \end{cases} \tag{27}$$

$\lambda_{3,\min})/\epsilon)$. It should be pointed out that significant computational saving can be achieved through the use of the proposed algorithms for large number of subcarriers and great MI threshold. Also, the gap goes up rapidly with the increase of the number of subcarriers and MI threshold.

IV. Robust OFDM Radar Waveform Design

In this section, we first introduce the uncertainty models for target spectra, and then propose the robust OFDM radar waveform design approaches to minimize the worst-case total transmit power under parameter uncertainties.

A. Uncertainty Models

Obtaining the optimal solutions of $\mathcal{P}_{\text{O-1}}$, $\mathcal{P}_{\text{O-2}}$ and $\mathcal{P}_{\text{O-3}}$ requires the target spectra $H_r[k]$, $H_s[k]$ and $H_e[k], k \in \mathcal{F}_k$. However, the perfect knowledge of these parameters is usually not available, which is because the exact target-radar/communication BS orientation is practically imprecise [29][31]. One approach is to utilize estimated values of the parameters in the waveform design strategies. Since these estimated values are subjected to uncertainty, the formulations $\mathcal{P}_{\text{O-1}}$, $\mathcal{P}_{\text{O-2}}$ and $\mathcal{P}_{\text{O-3}}$ may fail to provide reliable or feasible solutions. Furthermore, it is of high importance to control the power-saving performance loss to be within a certain bound. Thus, it is essential to develop robust waveform design methods to cope with the parameter uncertainty.

In realistic scenarios, the characteristics of the target spectra $H_r[k]$, $H_s[k]$ and $H_e[k], k \in \mathcal{F}_k$ can be obtained through electromagnetic modeling and calculation, and thus all are subject to uncertainty. We adopt robust signal processing methodology, which is developed in recent years to handle the optimization problems with parameter uncertainty [28][29]. Typically, the target spectra are assumed to lie in certain bounded sets, referred to as *uncertainty sets*. The upper and lower bounds can be obtained through field measurement or propagation modeling [28][29]. For illustrative purpose, the uncertainty set of target spectrum is shown in Fig.3, where the nominal target spectrum is illustrated by the blue bars, and the upper and lower bounds of the uncertainty set in each subcarrier are depicted by the error bars. Herein, we consider the actual target spectra to lie in linear uncertainty sets, i.e.:

$$\begin{cases} H_r[k] \in \mathcal{S}_{H_r} \triangleq \{l_r[k] \le H_r[k] \le u_r[k], k \in \mathcal{F}_k\}, \\ H_s[k] \in \mathcal{S}_{H_s} \triangleq \{l_s[k] \le H_s[k] \le u_s[k], k \in \mathcal{F}_k\}, \\ H_e[k] \in \mathcal{S}_{H_e} \triangleq \{l_e[k] \le H_e[k] \le u_e[k], k \in \mathcal{F}_k\}. \end{cases} \tag{29}$$

where $u_r[k]$, $u_s[k]$ and $u_e[k]$ denote the upper bounds of $H_r[k]$, $H_s[k]$ and $H_e[k]$ for the kth subcarrier, respectively. Likewise, $l_r[k]$, $l_s[k]$ and $l_e[k]$ denote the lower bounds of $H_r[k]$, $H_s[k]$ and $H_e[k]$ for the kth subcarrier, respectively. It should be pointed out that the distance between the upper and lower bounds at each subcarrier may be different. Also, note that a larger difference between the upper and lower bounds means greater uncertainty about the target [28].

Thus, as suggested by the robust signal processing theory described in [29], for the uncertainty sets, the robust radar waveform x_k^{robust} is the optimal waveform for the worst-case target spectra, i.e., $H_r[k] = H_r^{\text{worst}}[k]$, $H_s[k] = H_s^{\text{worst}}[k]$ and $H_e[k] = H_e^{\text{worst}}[k]$, $k \in \mathcal{F}_k$. If utilizing other waveforms, the power-saving performance of the radar system will be degraded; while if the robust radar waveform x_k^{robust} is utilized, the power-saving performance will be always as good as or better than the case $H_r[k] = H_r^{\text{worst}}[k]$, $H_s[k] = H_s^{\text{worst}}[k]$ and $H_e[k] = H_e^{\text{worst}}[k]$, $k \in \mathcal{F}_k$ for all target spectra in the uncertainty sets, which indicates that the achievable power-saving performance will never be worse than this limit. Hence, the robust waveform is optimum for the worst-case target spectra in the uncertainty sets.

B. Robust Radar Waveform Design Criterion 1

We employ the robust optimization methods to guarantee the worst-case power-saving performance in the presence of target spectra uncertainties. The worst-case MI due to target spectra uncertainties is shown in (30) [see (30) at the top of the next page]. Since the achievable MI in (12) is a monotonically increasing function of $H_r[k]$ and $H_s[k]$, the minimization of

$$\mathcal{I}^1_{\text{robust}}(\mathbf{y};\mathbf{H}_r,\mathbf{H}_s) \triangleq \min_{H_r[k]\in\mathcal{S}_{H_r},H_s[k]\in\mathcal{S}_{H_s},k\in\mathcal{F}_k} \left\{\sum_{k=0}^{K-1}\log\left(1+\frac{m_k x_k+a_k}{n_k x_k+b_k}\right)\right\}. \tag{30}$$

$$\overline{x}_k^* = \begin{cases} 0, & \lambda_3^*\widetilde{D}_k-\widetilde{C}_k\le 0,\\ -\frac{\widetilde{B}_k}{2\widetilde{A}_k}+\frac{1}{2\widetilde{A}_k}\sqrt{\widetilde{B}_k^2-4\widetilde{A}_k(\widetilde{C}_k-\lambda_3^*\widetilde{D}_k)}, & 0<\lambda_3^*\widetilde{D}_k-\widetilde{C}_k<A_k d_k^2+\widetilde{B}_k d_k,\\ d_k, & \lambda_3^*\widetilde{D}_k-\widetilde{C}_k\ge A_k d_k^2+\widetilde{B}_k d_k. \end{cases} \tag{36}$$

$$\mathcal{I}^2_{\text{robust}}(\mathbf{y};\mathbf{H}_r) \triangleq \min_{H_r[k]\in\mathcal{S}_{H_r},H_s[k]\in\mathcal{S}_{H_s},k\in\mathcal{F}_k} \left\{\sum_{k=0}^{K-1}\log\left(1+\frac{m_k x_k}{n_k x_k+a_k+b_k}\right)\right\}. \tag{39}$$

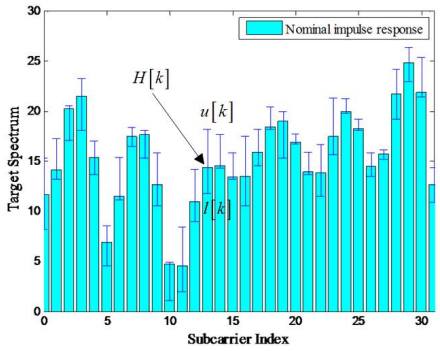

Fig. 3. Illustration of bounded target spectrum.

the achieved MI over $H_r[k]\in\mathcal{S}_{H_r}$ and $H_s[k]\in\mathcal{S}_{H_s}$ simply follows that:

$$\{l_r[k],l_s[k]\} \triangleq \arg\min_{H_r[k]\in\mathcal{S}_{H_r},H_s[k]\in\mathcal{S}_{H_s},k\in\mathcal{F}_k} \left\{\sum_{k=0}^{K-1}\log\left(1+\frac{m_k x_k+a_k}{n_k x_k+b_k}\right)\right\}. \tag{31}$$

Subsequently, we obtain $a_k=\underline{a}_k$ and $m_k=\underline{m}_k$, where

$$\begin{cases} \underline{a}_k=\sigma_{x_s}^2[k]|l_s[k]|^2L_s[k],\\ \underline{m}_k=|l_r[k]|^2L_r[k]. \end{cases} \tag{32}$$

On the other hand, however, the remaining maximization over $H_e[k]$ does not permit an explicit expression. It should be noticed that c_k is a monotonically decreasing function in $H_e[k]$. That is to say, c_k is reduced as $H_e[k]$ goes up. Then, with the increase of $H_e[k]$, c_k will become smaller than $P_{\max,k}$, thus we can have $d_k=c_k<P_{\max,k}$, i.e., the maximum transmit power at the kth subcarrier is decreased. This leads to the increase of λ_3^*, and thus, more transmit power will be allocated to guarantee the given MI constraint. The maximization over $H_e[k]\in\mathcal{S}_{H_e}$ can be achieved at $H_e[k]=u_e[k]$.

Hence, we replace a_k, m_k and $\mathbf{d}$ with $\underline{a}_k$, $\underline{m}_k$ and $\underline{\mathbf{d}}$ respectively in (15) and present a robust counterpart $\mathcal{P}_{\text{R-1}}$. Then, to guarantee the target characterization performance in the worst case, the problem of robust radar waveform design can be formulated as follows:

$$\mathcal{P}_{\text{R-1}}: \quad \min_{x_k,k\in\mathcal{F}_k}\sum_{k=0}^{K-1}x_k, \tag{33a}$$

$$\text{s.t.}: \begin{cases} \sum_{k=0}^{K-1}\log\left(1+\frac{\underline{m}_k x_k+\underline{a}_k}{n_k x_k+b_k}\right)\ge \text{MI}_{\min},\\ \mathbf{0}\le\mathbf{x}\le\underline{\mathbf{d}}. \end{cases} \tag{33b}$$

where

$$\begin{cases} \underline{c}_k=\frac{1}{u_e^2[k]L_e[k]}\left[\frac{\sigma_{x_s}^2[k]L_c[k]}{e^{t_k}-1}-\sigma_n^2[k]\right],\\ \underline{d}_k=\min\{P_{\max,k},\underline{c}_k\}. \end{cases} \tag{34}$$

Theorem 4: Suppose the target spectra lie in uncertainty sets bounded by known upper and lower bounds satisfying (29). Define

$$\begin{cases} \widetilde{B}_k=(\underline{m}_k+n_k)b_k+(\underline{a}_k+b_k)n_k,\\ \widetilde{C}_k=(\underline{a}_k+b_k)b_k,\\ \widetilde{D}_k=b_k\underline{m}_k-\underline{a}_k n_k. \end{cases} \tag{35}$$

The robust OFDM radar waveform corresponding to $\mathcal{P}_{\text{R-1}}$ that minimizes the total transmitted power under a predefined MI threshold and a minimum capacity for the communication system is the optimum waveform for any target spectra with samples $H_r[k]=l_r[k],H_s[k]=l_s[k],H_e[k]=u_e[k]$, for $k\in\mathcal{F}_k$. To be specific, the robust waveform uses (36), shown at the top of this page, where the constant λ_3^* is chosen now to satisfy:

$$\sum_{k=0}^{K-1}\log\left(1+\frac{\underline{m}_k\overline{x}_k^*+\underline{a}_k}{n_k\overline{x}_k^*+b_k}\right)\ge\text{MI}_{\min}. \tag{37}$$

Remark 4: Other formulations developed in Section III can also be extended to their robust formulations utilizing the above approach, where the target characterization performance is guaranteed to satisfy the MI requirement and the minimum capacity per channel for the communication system is maintained. However, if employing the non-robust formulations,

the requirements for the target estimation and the channel capacity in (13b) cannot be guaranteed due to the imperfect characteristics of target spectra.

C. Robust Radar Waveform Design Criterion 2

Now, we investigate the robust radar waveform design based on the optimal Criterion 2 $\mathcal{P}_{\text{O-2}}$. To circumvent the maximization of the total transmitted power, we consider the robust formulation, which can be written as follows:

$$\min_{x_k, k\in\mathcal{F}_k} \sum_{k=0}^{K-1} x_k, \tag{38a}$$

$$\text{s.t.}: \begin{cases} \mathcal{I}^2_{\text{robust}}(\mathbf{y};\mathbf{H}_r) \geq \text{MI}_{\min}, \\ \mathbf{0} \leq \mathbf{x} \leq \underline{\mathbf{d}}. \end{cases} \tag{38b}$$

where $\mathcal{I}^2_{\text{robust}}(\mathbf{y};\mathbf{H}_r)$ is shown at the top of the previous page. In this case, since the MI in (19) is a monotonically increasing function of $H_r[k]$ and a decreasing function of $H_s[k]$ respectively, the minimization of $\left\{\sum_{k=0}^{K-1}\log\left(1+\frac{m_k x_k}{n_k x_k + a_k + b_k}\right)\right\}$ over $H_r[k]\in\mathcal{S}_{H_r}$ and $H_s[k]\in\mathcal{S}_{H_s}$ is achieved at $H_r[k]=l_r[k]$ and $H_s[k]=u_s[k]$. Similarly, the problem (38) is equivalent to the following:

$$\mathcal{P}_{\text{R-2}}: \quad \min_{x_k, k\in\mathcal{F}_k} \sum_{k=0}^{K-1} x_k, \tag{40a}$$

$$\text{s.t.}: \begin{cases} \sum_{k=0}^{K-1}\log\left(1+\frac{\underline{m}_k x_k}{n_k x_k + \overline{a}_k + b_k}\right) \geq \text{MI}_{\min}, \\ \mathbf{0} \leq \mathbf{x} \leq \underline{\mathbf{d}}. \end{cases} \tag{40b}$$

where

$$\overline{a}_k = \sigma^2_{x_s}[k]|u_s[k]|^2 L_s[k]. \tag{41}$$

Theorem 5: Suppose the target spectra lie in uncertainty sets bounded by known upper and lower bounds satisfying (29). Define

$$\begin{cases} \widetilde{E}_k = (\underline{m}_k + 2n_k)(\overline{a}_k + b_k), \\ \widetilde{F}_k = (\overline{a}_k + b_k)^2, \\ \widetilde{G}_k = \underline{m}_k(\overline{a}_k + b_k). \end{cases} \tag{42}$$

The robust OFDM radar waveform corresponding to $\mathcal{P}_{\text{R-2}}$ that minimizes the total transmitted power under a predefined MI threshold and a minimum capacity for the communication system is the optimum waveform for any target spectra with samples $H_r[k]=l_r[k], H_s[k]=u_s[k], H_e[k]=u_e[k]$, for $k\in\mathcal{F}_k$. To be specific, the robust waveform uses (43), shown at the top of the next page, where the constant λ_3^* is chosen to satisfy:

$$\sum_{k=0}^{K-1}\log\left(1+\frac{\underline{m}_k \overline{x}_k^*}{n_k \overline{x}_k^* + \overline{a}_k + b_k}\right) \geq \text{MI}_{\min}. \tag{44}$$

D. Robust Radar Waveform Design Criterion 3

Similarly, the robust waveform design based on the optimal Criterion 3 $\mathcal{P}_{\text{O-3}}$ aims to solve:

$$\min_{x_k, k\in\mathcal{F}_k} \sum_{k=0}^{K-1} x_k, \tag{45a}$$

$$\text{s.t.}: \begin{cases} \mathcal{I}^3_{\text{robust}}(\mathbf{y};\mathbf{H}_r|\mathbf{H}_s) \geq \text{MI}_{\min}, \\ \mathbf{0} \leq \mathbf{x} \leq \underline{\mathbf{d}}. \end{cases} \tag{45b}$$

where $\mathcal{I}^3_{\text{robust}}(\mathbf{y};\mathbf{H}_r|\mathbf{H}_s)$ is shown at the top of the next page. Thus, (45) is equivalent to the following problem:

$$\mathcal{P}_{\text{R-3}}: \quad \min_{x_k, k\in\mathcal{F}_k} \sum_{k=0}^{K-1} x_k, \tag{47a}$$

$$\text{s.t.}: \begin{cases} \sum_{k=0}^{K-1}\log\left(1+\frac{\underline{m}_k x_k}{n_k x_k + b_k}\right) \geq \text{MI}_{\min}, \\ \mathbf{0} \leq \mathbf{x} \leq \underline{\mathbf{d}}. \end{cases} \tag{47b}$$

Theorem 6: Suppose the target spectra lie in uncertainty sets bounded by known upper and lower bounds satisfying (29). Define

$$\begin{cases} \widetilde{H}_k = b_k(\underline{m}_k + 2n_k), \\ \widetilde{J}_k = b_k^2, \\ \widetilde{L}_k = \underline{m}_k b_k. \end{cases} \tag{48}$$

The robust OFDM radar waveform corresponding to $\mathcal{P}_{\text{R-3}}$ that minimizes the total transmitted power under a predefined MI threshold and a minimum capacity for the communication system is the optimum waveform for any target spectra with samples $H_r[k]=l_r[k], H_e[k]=u_e[k]$, for $k\in\mathcal{F}_k$. To be specific, the robust waveform uses (49), shown at the top of the next page, where the constant λ_3^* is chosen to satisfy:

$$\sum_{k=0}^{K-1}\log\left(1+\frac{\underline{m}_k \overline{x}_k^*}{n_k \overline{x}_k^* + b_k}\right) \geq \text{MI}_{\min}. \tag{50}$$

E. Discussion

In all the robust OFDM radar waveform design criteria, the worst case is either the lower bounds or the upper bounds of the uncertainty sets of target spectra. Thus, the limitation can be reduced by employing either the lower bounds or the upper bounds of the target spectra uncertainty sets for all the criteria. Robust criteria are more concerned with the problem of how the radar waveform design schemes are affected by the target spectra uncertainty sets. Due to the fact that the objective of robust waveform design methods is to bound the worst-case power-saving performance, the robust radar waveforms are chosen based on the lower/upper bounds of the uncertainty sets of target spectra for all criteria.

V. Numerical Simulations and Analysis

In this section, simulation results are provided to verify the accuracy of the theoretical derivations as well as demonstrate the improvement of the power-saving performance brought by our proposed radar waveform design algorithms.

$$\overline{x}_k^* = \begin{cases} 0, & \lambda_3^*\widetilde{G}_k - \widetilde{F}_k \le 0, \\ -\frac{\widetilde{E}_k}{2\widetilde{A}_k} + \frac{1}{2A_k}\sqrt{\widetilde{E}_k^2 - 4A_k(\widetilde{F}_k - \lambda_3^*\widetilde{G}_k)}, & 0 < \lambda_3^*\widetilde{G}_k - \widetilde{F}_k < A_k d_k^2 + \widetilde{E}_k d_k, \\ d_k, & \lambda_3^*\widetilde{G}_k - \widetilde{F}_k \ge A_k d_k^2 + \widetilde{E}_k d_k. \end{cases} \tag{43}$$

$$\mathcal{I}^3_{\text{robust}}(\mathbf{y};\mathbf{H}_r|\mathbf{H}_s) \triangleq \min_{H_r[k]\in\mathcal{S}_{H_r},k\in\mathcal{F}_k} \left\{ \sum_{k=0}^{K-1} \log\left(1 + \frac{m_k x_k}{n_k x_k + b_k}\right) \right\}. \tag{46}$$

$$\overline{x}_k^* = \begin{cases} 0, & \lambda_3^*\widetilde{L}_k - \widetilde{J}_k \le 0, \\ -\frac{\widetilde{H}_k}{2\widetilde{A}_k} + \frac{1}{2A_k}\sqrt{\widetilde{H}_k^2 - 4A_k(\widetilde{J}_k - \lambda_3^*\widetilde{L}_k)}, & 0 < \lambda_3^*\widetilde{L}_k - \widetilde{J}_k < A_k d_k^2 + \widetilde{H}_k d_k, \\ d_k, & \lambda_3^*\widetilde{L}_k - \widetilde{J}_k \ge A_k d_k^2 + \widetilde{H}_k d_k. \end{cases} \tag{49}$$

TABLE I
CO-EXISTING RADAR AND COMMUNICATION SYSTEMS PARAMETERS

Parameter	Value	Parameter	Value
G_t	30 dB	G_r	40 dB
G_s	0 dB	d_r	20 km
d_s	15 km	d_c	5 km
d_b	20 km	$P_{\max,k}(\forall k)$	450 W
Δf	4 MHz	$\sigma_s^2[k]$	1.66×10^{-14} W

A. Numerical Setup

Throughout the simulations, the carrier frequency of the coexisting radar and communication system is 3 GHz. Here, we set the total bandwidth to be 512 MHz, which is equally divided by 128 subcarriers. In order for the communication system to function properly, the achievable capacity for each channel must be above a predetermined threshold, which is set to be $t_k = 1$ nat/symbol$(\forall k)$. The radar can access all the channels with a given MI performance constraint $\text{MI}_{\text{min}} = 2.5$ nats, which is approximately equivalent to the value of SINR $= 10.5$ dB for a specific target estimation requirement here [21][24]. We set the system parameters as given in TABLE I. To solve the optimal problems in $\mathcal{P}_{\text{O-1}}$, $\mathcal{P}_{\text{O-2}}$ and $\mathcal{P}_{\text{O-3}}$, it is assumed that the radar knows the precise characteristics of the target spectra, the propagation losses of corresponding channels and communication signals by sensing itself with a spectrum analyzer. While for the robust problems in $\mathcal{P}_{\text{R-1}}$, $\mathcal{P}_{\text{R-2}}$ and $\mathcal{P}_{\text{R-3}}$, the uncertainty sets of target spectra are similar to Fig.3, which are not shown for clarity.

B. Simulation Results

We consider a scenario that the target is illuminated from the front by the radar waveform and from the side by the communication signals. The power of corresponding channels h_r, h_s, and h_e are shown in Fig.4, respectively. The PSDs of the radar receiver noise and signal-dependent clutters associated with the radar signal and communication BS signal are depicted in Fig.5, where the clutters characteristics can be estimated by the radar receiver through previous received

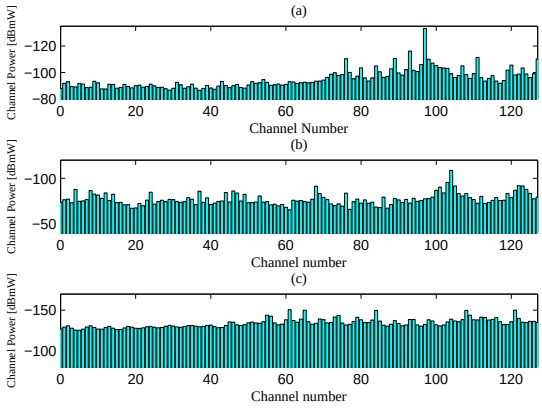

Fig. 4. The power of corresponding channels: (a) h_r; (b) h_s; (c) h_e.

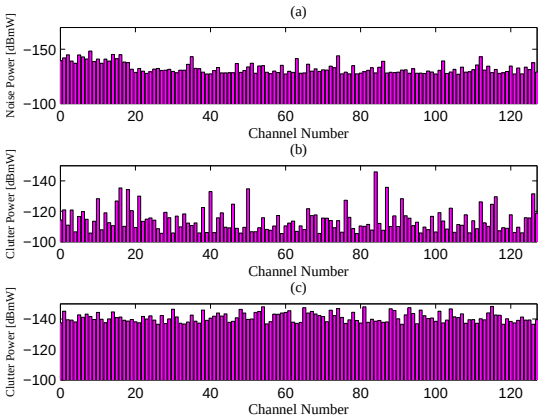

Fig. 5. The PSDs of colored noise and clutters: (a) Radar receiver noise; (b) Radar clutter; (c) Communication clutter.

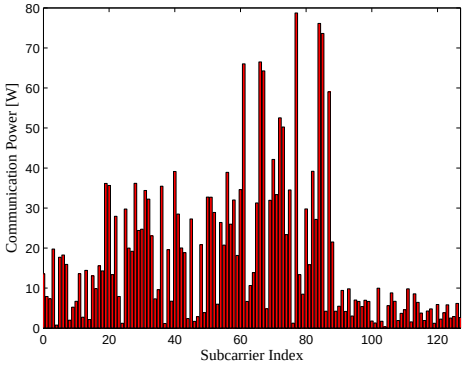

Fig. 6. Communication waveform.

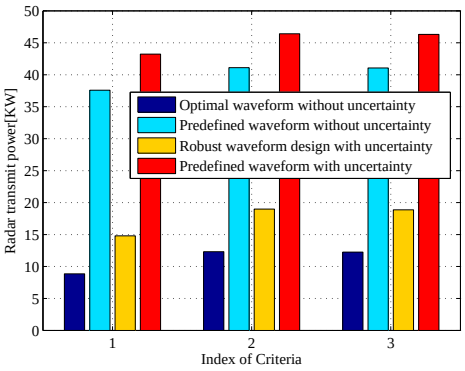

Fig. 8. Comparisons of radar transmit power using different algorithms.

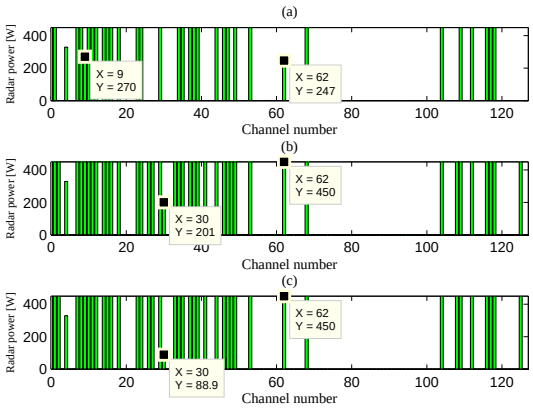

Fig. 7. Robust OFDM radar waveform design results: (a) $\mathcal{P}_{\text{R-1}}$; (b) $\mathcal{P}_{\text{R-2}}$; (c) $\mathcal{P}_{\text{R-3}}$.

signals. The communication waveform is illustrated in Fig.6. Fig.7 depicts the robust radar waveform design results, which give insight about the power allocation for the power-saving performance of radar system in the presence of target spectra uncertainties. Note that the optimal radar waveform results are similar to the robust results and are not illustrated. For all the criteria presented here, it can be observed that the transmit power allocation is determined by the target spectra and the communication waveform. To be specific, for the situation where the target spectrum $H_r[k]$ is weak while the interference power provided by the communication system is strong, we should concentrate less power for the subcarriers of radar transmitted waveform. While for the situation where $H_r[k]$ is large and the interference power is weak, we should allocate more power for the corresponding subcarriers of radar transmitted waveform. To minimize the total transmitted power for a predefined MI constraint and a minimum required capacity for the communication system, the robust radar waveform design criteria are formed by water-filling action, which only place the minimum power over the subcarriers with the largest gain and least interference power [30].

Fig.8 illustrates the comparisons of radar transmit power employing different algorithms, which is conducted 10^3 Monte-Carlo trials. One can see that the proposed optimal and robust waveform design algorithms enable us to reduce the radar transmit power to 25%-50% of that obtained by predefined waveforms with and without target uncertainty, in which the predefined waveforms allocate the transmit power uniformly in the whole frequency band. Furthermore, it should be noted that the power-saving performance of Criterion 1 outperforms that of the other two criteria, which is due to the fact that the communication signals scattered off the target would be a much more significant component in target parameter estimation than the radar signals [14]. Specifically, in Fig.7, more transmit power is allocated between the subcarrier 2 and 62 in Criteria 2 and 3 than that in Criterion 1. That is to say, if the communication signals scattered off the target are not considered for the alternative hypothesis of the Neyman-Pearson (NP) detector, the detected energy is reduced, resulting in a considerably lower target estimation performance. Therefore, we can conclude from Figs.4-8 that considering the scattering off the target due to the communication signals at the radar receiver significantly improves the target estimation performance, which in turn confirms that the power-saving performance of radar system benefits significantly from taking into consideration the communication signals scattered off the target at the radar receiver.

On the other hand, in robust Criterion 1, a system with $K = 1024$, $\epsilon = 0.1$, $\lambda_{3,\min} = 0$, $\lambda_{3,\max} = 10^5$, and $\lambda_3^* = 2.3145 \times 10^4$ would require only on the order of 2.55×10^3 iterations with the presented schemes, while the exhaustive search approach [37] requires on the order of 2.37×10^8 iterations. This indicates that the proposed algorithms require only $1.0759 \times 10^{-3}\%$ of the iterations compared with the exhaustive search method.

The total transmit power curves versus MI for each criterion are depicted in Fig.9. The total transmit power of the radar system when employing the optimal radar waveform for nominal target spectra, the robust radar waveform for the worst-case target spectra and the predefined radar waveform in the worst-case are compared in Fig.9. The best power-saving gain can be obtained when utilizing the optimal waveform in the best case, i.e., the nominal target spectra are used and the optimal radar waveform is designed assuming that the precise target spectra are known. It indicates that the radar transmits the minimum power for a predetermined MI threshold. The

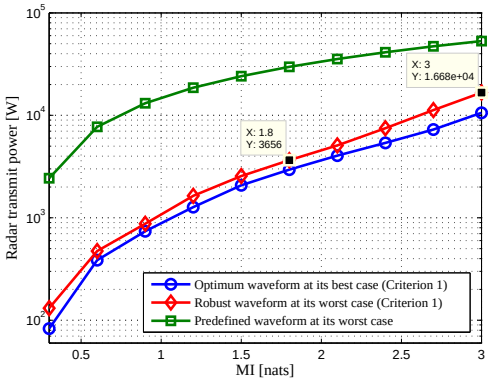

(a)

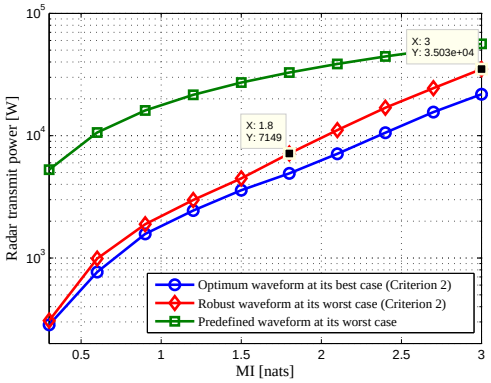

(b)

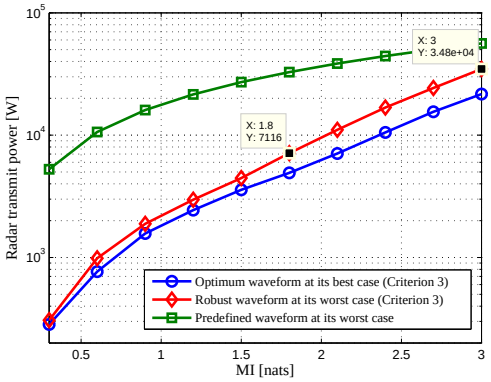

(c)

Fig. 9. Total transmit power of the radar system versus MI in each Criterion with different waveform design algorithms: (a) Criterion 1; (b) Criterion 2; (c) Criterion 3.

transmit power of the predefined waveform in the worst case is also provided. As aforementioned, the predefined waveform allocates the transmit power uniformly in the whole frequency band without any prior knowledge of the target spectra. It can be clearly observed that the predefined waveform exhibits a much inferior worst-case power-saving performance than that of the other waveforms. As expected, the robust radar waveform in the worst case is between the above two. This is due to the fact that the robust waveform design scheme has less prior knowledge about the target spectra. However, it is much better than the predefined waveform in the worst case, which optimizes the worst-case power-saving performance for the radar system [28][30]. Moreover, the robust Criterion 1 outperforms the robust Criteria 2 and 3 by 63.91% and 62.08%, respectively, when $\text{MI}_{\text{min}} = 3$ nats, which implies that the power-saving performance can be significantly enhanced by exploiting the communication signals scattered off the target at the radar receiver. Overall, the robust waveform effectively bounds the worst possible power-saving performance of the radar system over the entire uncertainty sets. If the robust radar waveform is employed, the power-saving performance will not be worse than this bound.

VI. Conclusion

In this paper, we have addressed the problem of power minimization based OFDM radar waveform design for spectrum sharing. Three different robust OFDM radar waveform design criteria are presented in the presence of target spectra uncertainties, which differ in the way the scattering off the target due to the communication signals is considered: (i) as useful energy, (ii) as interference or (iii) ignored altogether at the radar receiver. For each criterion, the worst-case radar transmit power is minimized and the associated optimization problem is formulated and solved analytically. With the aid of numerical simulations, it is demonstrated that the transmitted power of the radar system can be significantly decreased by exploiting the communication signals scattered off the target at the radar receiver. Moreover, the results also show that the robust waveforms can bound the worst-case power-saving performance at an acceptable limit. In future work, we will investigate the joint subcarrier and power allocation in OFDM radar systems. The radar waveform design problem taking into account the PAPR will also be studied in the future.

Appendix
Proof of Lemma 1

Proof: Since the contribution of each subcarrier's transmit power on the MI constraint is independent of the power of other subcarriers, that is,

$$\frac{\partial}{\partial x_l}\left[\log\left(1+\frac{m_k x_k + a_k}{n_k x_k + b_k}\right)\right] = 0, \forall k \neq l, \tag{51}$$

then, we have:

$$\frac{\partial}{\partial x_k}\left[\log\left(1+\frac{m_k x_k + a_k}{n_k x_k + b_k}\right)\right] = \frac{b_k m_k - a_k n_k}{(n_k x_k + b_k)[(m_k + n_k)x_k + a_k + b_k]}. \tag{52}$$

It can be noticed that whether the value of (52) is positive or not is relevant to a_k, b_k, m_k, and n_k. From (16), we know that $a_k > 0$, $b_k > 0$, $m_k > 0$, and $n_k > 0$, then:

$$(b_k m_k)/(a_k n_k) = \frac{|H_r[k]|^2 L_r[k](\sigma^2_{x_s}[k] L_d[k] + \sigma^2_{x_s}[k] P_{c_s}[k] L_{c_s}[k] + \sigma^2_n[k])}{P_{c_r}[k] L_{c_r}[k] \sigma^2_{x_s}[k] |H_s[k]|^2 L_s[k]}. \tag{53}$$

With $\sigma_n^2[k] > 0$, it can easily be shown that

$$\begin{aligned}
&(b_k m_k)/(a_k n_k) \\
&> \frac{|H_r[k]|^2 L_r[k](\sigma_{x_s}^2[k] L_d[k] + \sigma_{x_s}^2[k] P_{c_s}[k] L_s[k])}{P_{c_r}[k] L_r[k] \sigma_{x_s}^2[k] |H_s[k]|^2 L_s[k]} \\
&= \frac{|H_r[k]|^2 (L_d[k] + P_{c_s}[k] L_s[k])}{P_{c_r}[k] |H_s[k]|^2 L_s[k]} \\
&= \frac{|H_r[k]|^2 \left[(4\pi) \frac{d_s^2 d_r^2}{d_b^2} + P_{c_s}[k] \right]}{P_{c_r}[k] |H_s[k]|^2}.
\end{aligned} \tag{54}$$

According to the inequality $d_s + d_r > d_b$, we know that $(d_s + d_r)^2 > d_b^2$. Then, we can obtain

$$\begin{aligned}
(d_s + d_r)^2 &= d_s^2 + d_r^2 + 2 d_s d_r \\
&\geq 2\sqrt{d_s^2 d_r^2} + 2 d_s d_r \\
&= 4 d_s d_r > d_b^2.
\end{aligned} \tag{55}$$

With some mathematical derivation, we have

$$(4\pi) \frac{d_s^2 d_r^2}{d_b^2} > (4\pi) d_b^4 / (16 d_b^2) = \pi d_b^2 / 4. \tag{56}$$

Substituting (56) into (54), we can reformulate (54) as

$$\begin{aligned}
&(b_k m_k)/(a_k n_k) \\
&> \frac{|H_r[k]|^2 \left[(4\pi) \frac{d_s^2 d_r^2}{d_b^2} + P_{c_s}[k] \right]}{P_{c_r}[k] |H_s[k]|^2} \\
&> \frac{|H_r[k]|^2 (\pi d_b^2 / 4 + P_{c_s}[k])}{P_{c_r}[k] |H_s[k]|^2}.
\end{aligned} \tag{57}$$

As $d_b \gg$ 1km in practice, it is rational to achieve $|H_r[k]|^2 (\pi d_b^2/4 + P_{c_s}[k]) \geq P_{c_r}[k] |H_s[k]|^2$ for conventional air targets and clutter environments. Thus, $(b_k m_k)/(a_k n_k) > 1$. Then, we obtain

$$\frac{\partial}{\partial x_k} \left[\log \left(1 + \frac{m_k x_k + a_k}{n_k x_k + b_k} \right) \right] > 0, \tag{58}$$

and

$$\begin{aligned}
&\frac{\partial^2}{\partial x_k^2} \left[\log \left(1 + \frac{m_k x_k + a_k}{n_k x_k + b_k} \right) \right] \\
&= \frac{-(b_k m_k - a_k n_k)}{(n_k x_k + b_k)^2 [(m_k + n_k) x_k + a_k + b_k]^2} \\
&\quad \times [2 n_k (m_k + n_k) x_k + n_k a_k + 2 n_k b_k + m_k b_k] < 0,
\end{aligned} \tag{59}$$

$$\frac{\partial^2}{\partial x_k x_l} \left[\log \left(1 + \frac{m_k x_k + a_k}{n_k x_k + b_k} \right) \right] = 0, \forall k \neq l, \tag{60}$$

where equation (58) explains the increasing nature of the MI with respect to each x_k. Moreover, equations (59) and (60) show that the Hessian matrix of MI (12) with respect to $x_k, \forall k \in \mathcal{F}_k$ is a diagonal matrix with non-positive elements. Therefore, it is shown that $I_{\text{optimal}}(\mathbf{y}; \mathbf{H}_r, \mathbf{H}_s)$ is increasing and concave with respect to x_k (One can see from the above analysis that the value of d_b ensuring the concavity depends on the other system parameters. It should be noticed that the concavity of $I_{\text{optimal}}(\mathbf{y}; \mathbf{H}_r, \mathbf{H}_s)$ holds in most practical scenarios, while a sub-optimal solution can be provided when its concavity is not satisfied).

As a consequence, the MI constraint in (15b) constitutes a convex feasible set over $x_k, \forall k \in \mathcal{F}_k$, while the objective function is affine and the power constraint in (15b) is the intersection of $2K$ half-spaces, and hence convex [51][52]. This concludes the convex nature of the optimization problem $\mathcal{P}_{\text{O-1}}$, which completes the proof. ■

REFERENCES

[1] H. Y. Wang, J. T. Johnson, and C. J. Baker. *"Spectrum sharing between communications and ATC radar systems,"* IET Radar, Sonar & Navigation, 2017, 11(6): 994-1001.

[2] A. Aubry, A. D. Maio, Y. Huang, M. Piezzo, and A. Farina. *"A new radar waveform design algorithm with improved feasibility for spectral coexistence,"* IEEE Trans. on Aerospace and Electronic Systems, 2015, 51(2): 1029-1038.

[3] A. Aubry, V. Carotenuto, and A. D. Maio. *"Forcing multiple spectral compatibility constraints in radar waveforms,"* IEEE Signal Processing Letters, 2016, 23(4): 483-487.

[4] K. Gerlach. *"Thinned spectrum ultrawideband waveforms using stepped-frequency polyphase codes,"* IEEE Trans. on Aerospace and Electronic Systems, 1998, 34(4): 1356-1361.

[5] C. Nunn, and L. R. Moyer. *"Spectrally-compliant waveforms for wide-band radar,"* IEEE Aerospace and Electronic Systems Magazine, 2012, 27(8): 11-15.

[6] R. A. Romero, and K. D. Shepherd. *"Friendly spectrally shaped radar waveform with legacy communication systems for shared access and spectrum management,"* IEEE Access, 2015, 3: 1541-1554.

[7] K. W. Huang, M. Bica, U. Mitra, and V. Koivunen. *"Radar waveform design in spectrum sharing environment: Coexistence and cognition,"* IEEE Radar Conference (RadarCon), 2015: 1698-1703.

[8] M. Bica, and V. Koivunen. *"Generalized multicarrier radar: models and performance,"* IEEE Trans. on Signal Processing, 2016, 64(17): 4389-4402.

[9] C. Sturm, Y. L. Sit, M. Braun, and T. Zwick. *"Spectrally interleaved multi-carrier signals for radar network applications and multi-input multi-output radar,"* IET Radar, Sonar & Navigation, 2013, 7(3): 261-269.

[10] S. Sen, and A. Nehorai. *"Adaptive design of OFDM radar signal with improved wideband ambiguity function,"* IEEE Trans. on Signal Processing, 2010, 58(2): 928-933.

[11] G. Lellouch, A. K. Mishra, and M. Inggs. *"Stepped OFDM radar technique to resolve range and Doppler simultaneously,"* IEEE Trans. on Aerospace and Electronic Systems, 2015, 51(2): 937-950.

[12] S. Gogineni, M. Rangaswamy, and A. Nehorai. *"Multi-modal OFDM waveform design,"* IEEE Radar Conference (RadarCon), 2013: 1-5.

[13] M. Bica, K. W. Huang, U. Mitra, and V. Koivunen. *"Opportunistic radar waveform design in joint radar and cellular communication systems,"* IEEE Global Communications Conference (GLOBECOM), 2015: 1-7.

[14] M. Bica, K. W. Huang, V. Koivunen, and U. Mitra. *"Mutual information based radar waveform design for joint radar and cellular communication systems,"* IEEE International Conference on Acoustics, Speech and Signal Processing (ICASSP), 2016: 3671-3675.

[15] A. R. Chiriyath, B. Paul, G. M. Jacyna, and D. W. Bliss. *"Inner bounds on performance of radar and communications co-existence,"* IEEE Trans. on Signal Processing, 2016, 64(2): 464-474.

[16] B. Li, and A. Petropulu. *"Joint transmit designs for co-existence of MIMO wireless communications and sparse sensing radars in clutter,"* IEEE Trans. on Aerospace and Electronic Systems, 2017, DOI: 10.1109/-TAES.2017.2717518.

[17] S. D. Blunt, P. Yatham, and J. Stiles. *"Intrapulse radar-embedded communications,"* IEEE Trans. on Aerospace and Electronic Systems, 2010, 46(3): 1185-1200.

[18] D. Ciuonzo, A. D. Maio, G. Foglia, and M. Piezzo. *"Pareto-theory for enabling covert intrapulse radar-embedded communications,"* IEEE Radar Conference (RadarConf), 2015: 292-297.

[19] D. Ciuonzo, A. D. Maio, G. Foglia, and M. Piezzo. *"Intrapulse radar-embedded communications via multiobjective optimization,"* IEEE Trans. on Aerospace and Electronic Systems, 2015, 51(4): 2960-2974.

[20] P. M. Woodward. *"Information theory and the design of radar receivers,"* Proceedings of the IRE, 1951, 39(12): 1521-1524.

[21] M. R. Bell. *"Information theory and radar waveform design,"* IEEE Trans. on Information Theory, 1993, 39(5): 1578-1597.

[22] Y. Yang, and R. S. Blum. *"MIMO radar waveform design based on mutual information and minimum mean-square error estimation,"* IEEE Trans. on Aerospace and Electronic Systems, 2007, 43(1): 330-343.
[23] R. A. Romero, and N. A. Goodman. *"Waveform design in signal-dependent interference and application to target recognition with multiple transmissions,"* IET Radar, Sonar and Navigation, 2009, 3(4): 328-340.
[24] R. A. Romero, J. Bae, and N. A. Goodman. *"Theory and application of SNR and mutual information matched illumination waveforms,"* IEEE Trans. on Aerospace and Electronic Systems, 2011, 47(2): 912-927.
[25] Y. Chen, Y. Nijsure, Y. H. Chew, Z. Ding, and S. Boussakta. *"Adaptive distributed MIMO radar waveform optimization based on mutual information,"* IEEE Trans. on Aerospace and Electronic Systems, 2013, 49(2): 1374-1385.
[26] M. M. Naghsh, M. M. Hashemi, S. ShahbazPanahi, M. Soltanalian, and P. Stoica. *"Unified optimization framework for multi-static radar code design using information-theoretic criteria,"* IEEE Trans. on Signal Processing, 2013, 61(21): 5401-5416.
[27] C. Y. Chen, and P. P. Vaidyanathan. *"MIMO radar waveform optimization with prior information of the extended target and clutter,"* IEEE Trans. on Signal Processing, 2009, 57(9): 3533-3544.
[28] L. L. Wang, H. Q. Wang, K. K. Wong, and P. V. Brennan. *"Minimax robust jamming techniques based on signal-to-interference-plus-noise ratio and mutual information criteria,"* IET Communications, 2014, 8(10): 1859-1867.
[29] Y. Yang, and R. S. Blum. *"Minimax robust MIMO radar waveform design,"* IEEE Journal of Selected Topics in Signal Processing, 2007, 1(1): 147-155.
[30] C. G. Shi, F. Wang, M. Sellathurai, J. J. Zhou, and H. Zhang. *"Robust transmission waveform design for distributed multiple-radar systems based on low probability of intercept,"* ETRI Journal, 2016, 38(1): 70-80.
[31] B. Jiu, H. W. Liu, D. Feng, and Z. Liu. *"Minimax robust transmission waveform and receiving filter design for extended target detection with imprecise prior knowledge,"* Signal Processing, 2012, 92(1): 210-218.
[32] D. C. Schleher. *"LPI radar: fact or fiction,"* IEEE Aerospace and Electronic Systems Magazine, 2006, 21(5): 3-6.
[33] C. G. Shi, J. J. Zhou, and F. Wang. *"Adaptive resource management algorithm for target tracking in radar network based on low probability of intercept,"* Multidimensional Systems and Signal Processing, 2017, http://doi.org/10.1007/s11045-017-0494-8.
[34] B. Tang, M. M. Naghsh, and J. Tang. *"Relative entropy-based waveform design for MIMO radar detection in the presence of clutter and interference,"* IEEE Trans. on Signal Processing, 2015, 63(14): 3783-3796.
[35] Y. C. Liu, H. Y. Wang, and J. Wang. *"Robust multiple-input multiple-output radar waveform design in the presence of clutter,"* IET Radar, Sonar & Navigation, 2016, 10(7): 1249-1259.
[36] P. Setlur, and M. Rangaswamy. *"Waveform design for radar STAP in signal dependent interference,"* IEEE Trans. on Signal Processing, 2016, 64(1): 19-34.
[37] C. G. Shi, S. Salous, F. Wang, and J. J. Zhou. *"Low probability of intercept based adaptive radar waveform optimization in signal dependent clutter for joint radar and cellular communication systems,"* EURASIP Journal on Advances in Signal Processing, 2016, 2016(1): 1-13.
[38] G. Hakobyan, and B. Yang. *"A novel inter-carrier-interference free signal processing scheme for OFDM radar,"* IEEE Trans. on Vehicular Technology, 2017, DOI: 10.1109/TVT.2017.2723868.
[39] H. Ochiai, and H. Imai. *"On the distribution of the peak-to-average power ratio in OFDM signals,"* IEEE Trans. on communications, 2001, 49(2): 282-289.
[40] C. R. Berger, B. Demissie, J. Heckenbach, P. Willett, and S. L. Zhou. *"Signal processing for passive radar using OFDM waveforms,"* IEEE Journal of Selected Topics in Signal Processing, 2010, 4(1): 226-238.
[41] S. Lmai, A. Bourre, C. Laot, and S. Houcke. *"An efficient blind estimation of carrier frequency offset in OFDM systems,"* IEEE Trans. on Vehicular Technology, 2014, 63(4): 1945-1950.
[42] T. M. Schmidl, and D. C. Cox. *"Robust frequency and timing synchronization for OFDM,"* IEEE Trans. on Communications, 1997, 45(12): 1613-1621.
[43] A. B. Awoseyila, C. Kasparis, and B. G. Evans. *"Robust time-domain timing and frequency synchronization for OFDM systems,"* IEEE Trans. on Consumer Electronics, 2009, 55(2): 391-399.
[44] T. C. Wei, W. C. Liu, C. Y. Tseng, and S. J. Jou. *"Low complexity synchronization design of an OFDM receiver for DVB-T/H,"* IEEE Trans. on Consumer Electronics, 2009, 55(2): 408-413.
[45] T. H. Pham, S. A. Fahmy, and I. V. Mcloughlin. *"Efficient integer frequency offset estimation architecture for enhanced OFDM synchronization,"* IEEE Trans. on Very Large Scale Integration (VLSI) Systems, 2016, 24(4): 1412-1420.
[46] S. Attallah, Y. Wu, and J. Bergmans. *"Low complexity blind estimation of residual carrier offset in orthogonal frequency division multiplexing based wireless local area network systems,"* IET Communications, 2007, 1(4): 604-611.
[47] B. Park, H. Cheon, E. Ko, C. Kang, and D. Hong. *"A blind OFDM synchronization algorithm based on cyclic correlation,"* IEEE Signal Processing Letters, 2004, 11(2): 83-85.
[48] M. Tanda. *"Blind symbol-timing and frequency-offset estimation in OFDM systems with real data symbols,"* IEEE Trans. on Communications, 2004, 52(10): 1609-1612.
[49] A. Turlapaty, and Y. W. Jin. *"A joint design of transmit waveforms for radar and communications systems in coexistence,"* IEEE Radar Conference (RadarCon), 2014: 315-319.
[50] C. R. Berger, B. Demissie, J. Heckenbach, P. Willett, and S. L. Zhou. *"An overview of peak-to-average power ratio reduction schemes for OFDM signals,"* Journal of Communications and Networks, 2009, 11(3): 229-239.
[51] G. Alirezaei, O. Taghizadeh, and R. Mathar. *"Optimum power allocation with sensitivity analysis for passive radar applications,"* IEEE Sensors Journal, 2014, 14(11): 3800-3809.
[52] S. P. Boyd, and L. Vandenberghe. *"Convex optimization."* Cambridge University Press, 2004.

Chenguang Shi

Chenguang Shi was born in Luoyang, China, 1989. He received the B.S. and the Ph.D. degrees from Nanjing University of Aeronautics and Astronautics (NUAA), Nanjing, China, in 2012 and 2017, respectively. He is currently a lecturer at the Key Laboratory of Radar Imaging and Microwave Photonics (Nanjing Univ. Aeronaut. Astronaut.), Ministry of Education. His main research interests include low probability of intercept optimization, radar network, adaptive radar waveform design, and target tracking.

Fei Wang

Fei Wang received the M.S. degree and the Ph.D. degree from Jilin University in 2003 and 2006 respectively. He is currently a Associate Professor at NUAA.

His main research interests include aircraft radio frequency stealth, radar signal processing and array signal processing.

Mathini Sellathurai

Mathini Sellathurai (SMIEEE, FHEA) is a full Professor in Signal Processing and Intelligent Systems and Heriot-Watt University, Edinburgh, UK. In her 15-year research on Signal Processing for Communications, she has made seminal contributions on MIMO wireless systems. She has published 200 IEEE entries with 2300+ citations, given invited talks and has written a book and several book chapters in topics related to this project. She received the IEEE Communications Society Fred W. Ellersick Best Paper Award in 2005, Industry Canada Public Service Awards for contributions in science and technology in 2005, and Best PhD thesis award (Silver Medal) from NSERC Canada in 2002. She is also a member for IEEE SPCOM Technical Strategy Committee, Editor for IEEE TSP (2009-2014, 2015-present). She is also the General Co-Chair of IEEE SPAWC2016 in Edinburgh.

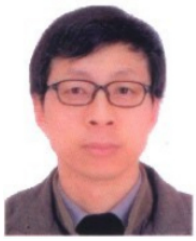

Jianjiang Zhou

Jianjiang Zhou received the M.S. degree and the Ph.D. degree from Nanjing University of Aeronautics and Astronautics (NUAA) in 1988 and 2001 respectively. He is currently a Professor and the Director of the Key Laboratory of Radar Imaging and Microwave Photonics (Nanjing Univ. Aeronaut. Astronaut.), Ministry of Education at NUAA.

His main research interests include aircraft radio frequency stealth, radar signal processing and array signal processing.

Sana Salous

Sana Salous (SM'95) received the B.E.E. degree from the American University of Beirut, Beirut, Lebanon, in 1978, and the M.Sc. and Ph.D. degrees from Birmingham University, Birmingham, U.K., in 1979 and 1984, respectively.

She was an Assistant Professor with Yarmouk University, Irbid, Jordan, for four years. She was a Research Fellow with Liverpool University, Liverpool, U.K., for one year. She held a lectureship with the University of Manchester Institute of Science and Technology, Manchester, U.K., in 1989, where she was subsequently a Senior Lecturer and then a Reader. Since 2003, she has been the Chair in Communications Engineering with Durham University, Durham, U.K., where she is currently the Director of the Centre for Communication Systems. Her current research interests include radio channel characterization in various frequency bands ranging from skywave in the HF band to millimeter bands at 60 GHz, the design of radar waveforms, and novel radio channel sounders and radar systems for radio imaging.

Dr. Salous is a fellow of the Institution of Engineering and Technology. She is the Chair of the Commission C on Radio Communication and Signal Processing Systems of the International Union of Radio Science. She is an Associate Editor of the Radio Science journal.